Carbohydrate Polymers 96 (2013) 71–81

Contents lists available at SciVerse ScienceDirect

Carbohydrate Polymers

journal homepage: www.elsevier.com/locate/carbpol

Mechanical and water barrier properties of agar/κ-carrageenan/konjac glucomannan ternary blend biohydrogel films

Jong-Whan Rhim*, Long-Feng Wang

Department of Food Engineering, Mokpo National University, 61 Dorimri, Chungkyemyon, Muangun, 534-729 Jeonnam, Republic of Korea

ARTICLE INFO

Article history:
Received 26 February 2013
Received in revised form 25 March 2013
Accepted 26 March 2013
Available online 3 April 2013

Keywords:
Agar
κ-Carrageenan
Konjac glucomannan
Ternary blend film
Clay nanocomposite
Hydrogel

ABSTRACT

Multicomponent hydrogel films composed of agar, κ-carrageenan, konjac glucomannan powder, and nanoclay (Cloisite® 30B) were prepared and their mechanical and water barrier properties such as water vapor permeability (WVP), water contact angle (CA), water solubility (WS), water uptake ratio (WUR), water vapor uptake ratio (WVUR) were determined. Mechanical, water vapor barrier, and water resistance properties of the ternary blend film exhibited middle range of individual component films, however, they increased significantly after formation of nanocomposite with the clay. Especially, the water holding capacity of the ternary blend biopolymer films increased tremendously, from 800% to 1681% of WUR for agar and κ-carrageenan films up to 5118% and 5488% of WUR for the ternary blend and ternary blend nanocomposite films, respectively. Water vapor adsorption behavior of films was also tested by water vapor adsorption kinetics and water vapor adsorption isotherms test. Preliminary test result for fresh spinach packaging revealed that the ternary blend biohydrogel films had a high potential for the use as an antifogging film for packaging highly respiring agricultural produce. In addition, the ternary blend nanocomposite film showed an antimicrobial activity against Gram-positive bacteria, *Listeria monocytogenes*.

1. Introduction

Hydrogels are highly hydrophilic polymer gels with macromolecular three dimensional networks that swell by absorbing and retaining large amounts of water without dissolving or losing their integrity in water (Farris, Schaich, Liu, Piergiovanni, & Yam, 2009; Kopeček & Yang, 2007). Structurally, they are polymers crosslinked via chemical interactions such as covalent bonds, ionic interactions, and hydrogen bonds, physical interactions such as coordinative, electrostatic, hydrophobic, and dipole–dipole interactions, or chain entanglements between the network segments (Mateescu, Wang, Dostalek, & Jonas, 2012). Generally, they are classified as natural and synthetic hydrogels based on their source; physical hydrogels, chemical hydrogels, and interpenetrating polymer networks based on their polymer interaction mechanism; degradable and non-degradable hydrogels based on their biodegradability (Farris et al., 2009; Kopeček & Yang, 2007; Mateescu et al., 2012). Hydrogels have wide range of applications such as membranes (Xu, Bartley, & Johnson, 2003), superabsorbent pads (Fernández, Picouet, & Lloret, 2010; Wu, Deng, & Lin, 2013; Yadav & Rhee, 2012), biosensors (Fernández, López, López-Cabarcos, & Mijangos, 2005; Mateescu et al., 2012; Zhang, Guan, & Zhang, 2012), encapsulation of bioactive compounds (Jen, Wake, & Mikos, 1996; Öztop, Hepokur, & Saraydin, 2009), largely in the biomedical field (contact lens, wound dressing, tissue engineering, drug delivery, etc.) (Berger et al., 2005; Liu & Chan-Park, 2009; Ma and Tu, 2010; Pourjavadi & Barzegar, 2009; Wang et al., 2012; Yu, Xu, Chen, Hao, & Jing, 2006), and for food packaging as well (Farris et al., 2009; Roy, Saha, Kitano, & Saha, 2012). Hydrogels can be prepared from a wide variety of materials, of natural origin, obtained from microorganisms, plants, and animals, as well as from materials prepared by modification or blending of aforementioned natural structures and from synthetic polymeric materials with various crosslinkers (Farris et al., 2009; Gibas & Janik, 2010; Hennink, & van Nostrum, 2002; Mateescu et al., 2012). Among the synthetic polymeric hydrogels, acrylate derivatives such as poly([meth/]acrylic acid) and poly([meth/]/acrylamide) have been frequently used due to their high water holding capacity with good optical, mechanical, and gas barrier properties (Kundakci, Üzüm, & Karadağ, 2008; Mateescu et al., 2012; Okay, Sariişik, & Zor, 1998; Öztop et al., 2009; Zhang, & Zhuo, 2002). However, most of the plastic materials are practically neither biodegradable nor biocompatible. In addition, polyacrylamide and acrylamide residues in the polyacrylamide-based hydrogels might cause probable health hazards (Andersen, 2005;

* Corresponding author. Tel.: +82 61 450 2423; fax: +82 61 454 1521.
E-mail addresses: jwrhim@mokpo.ac.kr, jwrhim@hanmail.net (J.-W. Rhim).

0144-8617/$ – see front matter © 2013 Elsevier Ltd. All rights reserved.
http://dx.doi.org/10.1016/j.carbpol.2013.03.083

Yener & Kalipci, 2009). As an alternative for the non-biodegradable synthetic plastic materials, biopolymers produced from various natural resources, such as starch, cellulose, and proteins, have been considered since they are abundant, renewable, inexpensive, environmentally friendly, and biocompatible (Luckachan & Pillai, 2011; Siracusa, Rocculi, Romani, & Rossa, 2008). However, there are some limitations to the commercial use of biopolymer films due to their poor mechanical properties and high sensitivity to moisture (Cabedo, Feijoo, Villanueva, Lagarón, & Giménez, 2006; De Azeredo, 2009; Luckachan & Pillai, 2011). Various efforts have been made to overcome these problems and to improve the property of biopolymer-based films through not only physical, chemical, or enzymatic treatments, but also blending with hydrophobic additives or other biopolymers (Cabedo et al., 2006; Luckachan & Pillai, 2011; Rhim, 2012). Recently, nanocomposite technology, compositing biopolymer with layered silicate clay materials such as montmorillonite, has been tested to improve the biopolymeric film properties (Bordes, Pollet, & Avérous, 2009; De Azeredo, 2009; Rhim, & Ng, 2007). Generally, hydrogels with improved properties can be obtained by blending with more than two polymers, in which polymer–polymer interactions can be strengthened by combining biopolymers with different structures introducing predominantly charge interactions rather than hydrogen bonding (Farris et al., 2009).

The bio-hydrogels with improved physicochemical properties can offer new opportunities for the design of efficient biopolymer-based biodegradable and/or biocompatible polymeric materials with desirable properties. Though the earliest and most widely used applications of hydrogels are in medicine and pharmaceutics (Kopeček & Yang, 2007), much less attention has been paid to the use of bio-hydrogel films for the food packaging application.

The main objectives of this study were to prepare highly water absorbing hydrogel films by blending with biopolymers, such as agar, κ-carrageenan, and konjac glucomannan powder, and nanoclay (Cloisite® 30B) through the solvent casting method to improve mechanical and water resistant properties of the blended hydrogel film and to test their applicability as a food packaging material.

2. Materials and methods

2.1. Materials

Food grade agar and κ-carrageenan, and konjac powder were obtained from Fine Agar Agar Co., Ltd. (Damyang, Jeonnam, Korea), Hankook Carragen (Whasoon, Jeonnam, Korea), and Milyang Agar Co., Ltd. (Milyang, Kyungnam, Korea), respectively. Organically modified nanoclay (Cloisite® 30B) was procured from Southern Clay (Gonzales, TX, USA) and glycerol was purchased from Daejung Chemicals & Metals Co., Ltd. (Siheung, Gyonggido, Korea). Nine analytical reagent grade salts (LiCl, CH_3COOK, $MgCl_2$, K_2CO_3, $Mg(NO_3)_2$, KI, NaCl, KCl, and KNO_3) were used for the preparation of saturated salt solutions.

2.2. Preparation of films

Three different polysaccharide-based films, agar, κ-carrageenan, and konjac, and their ternary blend films with and without nanoclay (Cloisite® 30B) were prepared using a solvent casting method (Rhim, Lee, & Hong, 2011). For the preparation of single component film solution, three grams of each of agar, κ-carrageenan, and konjac powder were dissolved in a constantly stirred mixture of distilled water (150 mL) and glycerol (30 wt% of solid, 0.9 g) with heating above 90 °C for 30 min. The ternary blend film solution was prepared by dissolving 1 gram of each polysaccharide powder with 30 wt% of glycerol and followed the same procedure. And the ternary blend/clay nanocomposite film solution was prepared according to the method described by Rhim et al. (2011). In short, precisely weighed nanoclay (5 wt% of biopolymers) was first dispersed into distilled water (150 mL) and swelled by stirring using a magnetic stirrer for 24 h, then homogenized using a high shear mixing homogenizer (T25 basic, Ika Labotechnik, Janke & Kunkel Gmbh & Co., KG Staufen, Germany) at 20,500 rpm for 10 min, and followed by sonication for 10 min using a high-intensity ultrasonic processor (Model VCX 750, Sonics & Materials Inc., Newtown, CT, USA). Then one gram each of agar and κ-carrageenan, and konjac powder were dissolved into the nanoclay solution then heating the mixture at 95 °C for 30 min with constant stirring and added 0.9 g of glycerol. The film solutions were cast onto a glass plate (24 × 30 cm) coated with Teflon layer (Cole-Parmer Instrument Co., Chicago, IL, USA). The cast films were dried for about 24 h at room temperature (2261 ± 2 °C), and then peeled off from the casting surface. The ternary blend films prepared with and without nanoclays were marked as A/C/K and A/C/K/Clo30B films, respectively.

2.3. Film thickness and conditioning

Film thickness was measured using a micrometer (Dial Thickness gauge 7301, Mitutoyo, Japan) with an accuracy of 0.01-mm. All film samples were preconditioned in a constant temperature humidity chamber set at 25 °C and 50% RH for at least 48 h before further test.

2.4. Color and transparency

Surface color of the films was measured using a Chroma meter (Konica Minolta, CR-400, Tokyo, Japan). A white standard color plate ($L = 97.75$, $a = -0.49$ and $b = 1.96$) was used as a background for color measurements. Hunter color (L, a and b) values were averaged from five readings from each sample. The total color difference (ΔE) was calculated as follows:

$$\Delta E = \sqrt{(\Delta L)^2 + (\Delta a)^2 + (\Delta b)^2} \quad (1)$$

where ΔL, Δa, and Δb are difference between each color values of standard color plate and film specimen, respectively.

The percent transmittance at wavelength of 660 nm (T_{660}) was determined using a UV/vis spectrophotometer (Model 8451A, Hewlett-Packard Co., Santa Alara, CA, USA) (Rhim, Hong, Park, & Ng, 2006).

2.5. Mechanical properties

The mechanical properties of the films including the tensile strength (TS), elongation at break (EB), and elasticity of modulus (E) were determined according to the standard ASTM method D 882-88 using an Instron Universal Testing Machine (Model 5565, Instron Engineering Corporation, Canton, MA, USA) equipped with a 0.5 kN load cell. Rectangular strips (2.54 × 10 cm) were cut from individually prepared film using a precision double blade cutter (model LB.02/A, Metrotec, S.A., San Sebastian, Spain). Initial grip separation was set at 50 mm and cross-head speed at 50 mm/min. The TS (MPa) was determined by dividing the maximum load (N) by the initial cross-sectional area (m^2) of the film sample, the EB (%) was determined by dividing the extension at rupture of the film (L) by the initial length of the film (L_o; 50 mm) multiplied by 100, and the E (σ/ε, GPa) was determined from the slope of linear portion of the stress–strain curve, which corresponds to the stress ($\sigma = F/A$) divided by the strain ($\varepsilon = L/L_o$) of the film samples.

2.6. Water vapor permeability (WVP)

The WVP of film was determined using a gravimetric method in accordance with the ASTM E-96-95 standard method. Water vapor transmission rate (WVTR) of film sample was determined gravimetrically at 25 °C under 50% RH conditions using water vapor transmission measuring cups as described by Gennadios, Weller, and Gooding (1994). The WVTR (water vapor mass flux in g/m^2 s) was calculated by the linear regression from the linear portion of the weight change vs. time curve. Then the WVP (g m/m^2 s Pa) of the film was calculated using the following equation:

$$\mathrm{WVP} = \frac{(\mathrm{WVTR} \times \mathrm{L})}{\Delta p} \quad (2)$$

where L was the mean film thickness (m) and Δp was the partial water vapor pressure difference (Pa) across the two sides of the film, which was corrected by the method proposed by Gennadios et al. (1994).

2.7. Water contact angle (CA)

The contact angle of water in air on the film surface was measured using a CA analyzer (Model Phoenix 150, Surface Electro Optics Co., Ltd., Kunpo, Korea) after a water drop of ca. 10 μL was placed on the surface of film using a micro syringe as described by Rhim et al. (2011).

2.8. Water resistance

Water solubility (WS) of films was determined as the percentage of soluble matter to the initial dry matter of film sample (Rhim, 2011). Three randomly selected specimens from each type of film were first dried at 105 °C for 24 h to determine initial dry matter. Separate films were immersed in 30 mL of distilled water in a 50 mL beaker. Beakers were covered with Parafilm "M" wrap (American National Can, Greenwich, CT) and stored in an environmental chamber at 25 °C for 30 min with occasional stirring. Undissolved dry matter was determined by removing the film pieces from the beakers, gently rinsing them with distilled water, and then oven drying them (105 °C, 24 h). The weight of solubilized matter was calculated by subtracting the weight of unsolubilized dry matter from the weight of initial dry matter and expressed as a percentage of the initial dry matter content.

Water uptake ratio (WUR) of films was determined gravimetrically. Pre-weighed squared specimens (25.4 mm × 50 mm) were immersed in distilled water for 30 min. Samples were then removed and weighed after removing the surface water with blotting paper. The WUR was calculated as follows:

$$\mathrm{WUR}\ (\%) = \frac{m_t - m_o}{m_o} \times 100. \quad (3)$$

where m_o and m_t are the weight of the samples before and after immersion, respectively.

Water vapor uptake ratio (WVUR) was determined following the method of Rhim (2011). Squared samples (25.4 mm × 50 mm) were first dried in a vacuum drier at 60 °C for 1 day. After being weighed using a four-digit electronic balance, the samples were stored over KNO_3 saturated salt (98% RH) at a constant temperature chamber of 25 °C for 24 h, and then weighed the samples after water vapor adsorption. The WVUR was calculated as:

$$\mathrm{WUR}\ (\%) = \frac{m_t - m_o}{m_o} \times 100 \quad (4)$$

where m_o and m_t are the weight of the samples before and after water vapor adsorption, respectively.

2.9. Water vapor adsorption kinetics

Water vapor adsorption of the film samples was determined by a gravimetric method at three different temperatures (10, 25, and 40 °C) using the method of Kim and Rhim (2004). Saturated potassium nitrate solution, which was contained in the Fido airtight glass jar with a compressed silicone gasket and clamp lid (1.0 L, Bormioli Rocco & Figllo SpA, Fidenza, Italy), was used to obtain constant relative humidity of the environment at each temperature. About 0.1 g of each film sample was placed on a sample holder made of stainless steel wire mesh which was placed on a tripod in the airtight glass jar. The unit was kept in a constant temperature chamber which was maintained within 61 ± 0.5 °C of the indicated temperature. The RH inside the glass jars are 0.96061 ± 0.014%, 0.93661 ± 0.006%, and 0.89061 ± 0.012%, respectively (Bell & Labuza, 2000). Increase in weight of the film specimens during the water vapor adsorption process was recorded intermittently until they reached saturated condition. Then water vapor adsorption curves were obtained by plotting the increase in weight due to water vapor adsorption (g H_2O/g DM) against adsorption time (min). The rate constant of water vapor adsorption (k) and the equilibrium moisture content (m_e) at each condition of film samples were determined using a linearized model of Singh and Kulshrestha (1987):

$$\frac{1}{m - m_o} = \frac{1}{k(m_\theta - m_o)t} + \frac{1}{m_\theta - m_o} \quad (5)$$

where m_o and m_e are the initial and the saturation (or equilibrium) moisture content, respectively.

2.10. Water vapor adsorption isotherms

Water vapor adsorption isotherms of films were determined using the static gravimetric method (Rhim, 2011). Nine saturated salt solutions (LiCl, CH_3COOK, $MgCl_2$, K_2CO_3, $Mg(NO_3)_2$, KI, NaCl, KCl, and KNO_3) were used to maintain constant water activities ranging from 0.11 to 0.96 at three temperatures, 10, 25, and 40 °C (Bell & Labuza, 2000). In each of 9 sealed glass bottles, the film samples (2.54 cm × 5 cm) were placed at different constant water activity established using the saturated salt solutions, and equilibrium moisture content was measured after 20 days at a constant temperature. Three replications were made at each water activity and average values of moisture content were used for constructing the isotherm curves. The GAB model was used to fit the water vapor adsorption data of the film samples. The GAB model contains three parameters as follows:

$$m = \frac{m_o C k a_w}{(1 - k a_w)(1 - k a_w + C k a_w)} \quad (6)$$

where m is the equilibrium moisture content (on dry weight basis) at water activity, a_w; m_o is the moisture content of monolayer corresponding to formation of a mono-molecular layer on the internal surface of the film samples; C is the Guggenheim constant; and k is a factor corresponding properties of the multilayer molecules with respect to the bulk liquid.

The GAB model parameters (m_o, C and k) were estimated by a non-linear regression method employing the Marquardt–Levenberg algorithm using the Solver function of Excel® (Billo, 2007) and the goodness of fit of the GAB model to the experimental equilibrium moisture content and water activity data was evaluated based on the mean relative percent errors (MRPE) as follows:

$$\mathrm{MRPE} = \frac{100}{n} \sum_{i=1}^{n} \frac{|m_i - m_{pi}|}{m_i} \quad (7)$$

Table 1
Apparent surface color and transmittance of agar, κ-carrageenan, konjac glucomannan, and their blend films.[a]

Film[b]	*L*	*a*	*b*	ΔE	$T_{660\,nm}$ (%)
Agar	92.61 ± 0.21b	−0.4261 ± 0.01c	4.8561 ± 0.05b	2.6461 ± 0.17b	86.1761 ± 1.03d
κ-Carrageenan	93.3061 ± 0.10c	−0.3461 ± 0.02d	3.7461 ± 0.08a	1.4061 ± 0.12a	89.2861 ± 0.37e
Konjac glucomannan	92.2461 ± 0.22a	−0.6361 ± 0.03a	6.0061 ± 0.22c	3.7461 ± 0.28d	78.8861 ± 1.08b
A/C/K[b]	92.7261 ± 0.09b	−0.4861 ± 0.02b	4.7661 ± 0.09b	2.4961 ± 0.12b	84.3761 ± 0.44c
A/C/K/Clo30B[b]	92.6661 ± 0.15b	−0.6161 ± 0.02a	5.8961 ± 0.23c	3.4161 ± 0.27c	50.8461 ± 0.82a

[a] Each value is the mean of three replicates with the standard deviation. Any two means in the same column followed by the same letter are not significantly ($p > 0.05$) different by Duncan's multiple range test.
[b] A/C/K, agar/κ-carrageenan/konjac glucomannan ternary blend film; Clo30B, Cloisite® 30B.

where m_i is the experimental moisture content; m_{pi} is the predicted moisture content and n is number of experimental points. The MRPE has been widely adopted through literature to evaluate the goodness of fit of sorption models, and an MRPE value less than 10% indicates a good fit for practical purposes (Zeppa, Gouanve, & Espuche, 2009).

2.11. Antimicrobial activity

Antimicrobial activity of the films against *Listeria monocytogenes* (ATCC-19111) was tested using a viable cell count method (Rhim et al., 2006). Film samples were cut into square pieces (10 × 10 cm) and placed in individual sterile flasks. The bacteria were incubated separately in brain heart infusion (BHI) broth (Difco Laboratories Inc., Detroit, MI, USA) at 37 °C under aerobic conditions for 16 h. One hundred milliliters of 1/10 diluted old cultured broth ($2.6–3.0 \times 10^4$ CFU/ml) was aseptically transferred to the flasks containing the test films. An inoculum of cell suspension in a flask without a test film was used as a control. The cell in the flask was incubated at 30 °C using an orbital shaker and rotated at 30 rpm. Aliquots of 0.1 mL of cell suspension was periodically taken from the flask, serially diluted, and plated on appropriate agar plates and subsequently incubated at 37 °C and 30 °C for 2 days. Each experiment was performed in triplicates and the results were presented as the mean 61 ± SD values in CFU/mL.

2.12. Packaging test

To test the antifogging effect of the hydrogel films, a storage test was performed by packaging a highly respiring agricultural produce, spinach. Fifty grams of fresh spinach purchased at a local market was packaged in a PP tray (size: 12 cm × 17.5 cm × 5 cm; thickness: 400 μm) and covered with different films, i.e., without cover for the control test, LLDPE (thickness: 10 μm, 3 M Fresh wrap, Ilshin Chemical Co., Ltd., Ansan, Korea), OPP (thickness: 60 μm, Samyoung Chemical Co., Ltd., Pusan, Korea), perforated OPP (perforation ratio: 1%), A/C/K, and A/C/K/Clo30B films. The packaged spinach samples were stored in a constant temperature chamber controlled at 5 °C for 5 days and observed surface of the covered film to check the antifogging effect of the packaged film, then weighed the spinach to determine the weight loss after storage.

2.13. Statistical analysis

Measurements of each property of films and storage tests were performed in triplicate with individually prepared film samples as the replicated experimental units, and mean values with standard deviations (SD) were reported. One-way analysis of variance (ANOVA) was performed, and the significance of each mean property value was determined ($p < 0.05$) with the Duncan's multiple range test using the SPSS statistical analysis computer program for Windows (SPSS Inc., Chicago, IL, USA).

3. Results and discussion

3.1. Apparent film properties

Gel is a viscoelastic solid-like material forming a polymer network dispersed in a continuous gas or liquid medium and is called either aerogel (highly porous) or xerogel (dehydrated), and hydrogel when a dispersing mediums are gas and water, respectively (Mateescu et al., 2012). Clear and flexible free-standing xerogel type films were obtained when all the film preparation solutions were cast and dried. However, the clay nanocomposite blend (A/C/K/Clo30B) film was slightly translucent. Apparent color and transparency properties of agar, κ-carrageenan, and konjac glucomannan films and their ternary blend films are shown in Table 1. Apparent color determined by Hunter *Lab*-values and transparency determined by percent transmittance at 660 nm (T_{660}) of the three biopolymer films indicate that the lightness (*L*-value), greenness (*a*-value), blueness (*b*-value), and transmittance (T_{660}) were the highest in the κ-carrageenan film, followed by the agar and konjac glucomannan films, respectively. Generally, the apparent color values of the ternary blend biopolymer films exhibited the color values depending on the individual component polymer. However, the nanoclay composited biopolymer blend film (A/C/K/Clo30B) exhibit a significantly ($p < 0.05$) decreased transmittance. It is mainly because the dispersed clay nanoparticles in the polymer matrix prevent the passage of light. This explains the apparent translucence of the nanocomposite film.

3.2. Mechanical properties

The mechanical properties of agar, κ-carrageenan, konjac glucomannan, and their blend films are shown in Table 2. Among the three biopolymers, the κ-carrageenan film showed the highest mechanical strength with the TS of 70.1261 ± 6.15 MPa and followed by the agar and konjac glucomannan films. The TS of κ-carrageenan and agar films showed much higher than those previously reported ones for 39.3461 ± 0.51 and 31.0361 ± 0.74 MPa, respectively (Rhim, 2012). This difference is mainly attributed to the fact that a less amount of plasticizer (30 wt% of glycerol) was used in the present study compared with 50 wt% of glycerol in the previous study. Glycerol acts as a plasticizer without forming any covalent linkages with the biopolymer. The hydroxyl groups present in glycerol are expected to form hydrogen bond with the biopolymer molecules at carbonyl and hydroxyl sites. Being small in size, it effectively increases the free volume of the system, thus decreasing the glass transition temperature and intermolecular forces. As a result, the plasticized biopolymer matrix changes from brittle to leathery to rubber with increased flexibility and extensibility of the film, as the concentration of glycerol is increased. The stiffness of the films determined by the Young's modulus (*E*) was followed the same order as the TS, while the flexibility of the films exhibited by the elongation at break (EB) showed the reversed order. As expected, all the mechanical properties of the ternary blend (A/C/K) film were in-between ranges of those of the

Table 2
Tensile properties of agar, κ-carrageenan, konjac glucomannan, and their blend films.[a]

Film	Thickness (μm)	TS (MPa)	EB (%)	*E* (GPa)
Agar	41.461 ± 0.9a	46.361 ± 2.4b	22.461 ± 3.1c	1.5761 ± 0.63b
κ-Carrageenan	39.861 ± 1.0a	70.161 ± 6.2d	10.761 ± 2.4a	2.5561 ± 0.23d
Konjac glucomannan	63.661 ± 5.6c	34.861 ± 2.0a	48.161 ± 4.8d	0.7261 ± 0.24a
A/C/K[b]	47.861 ± 2.2b	62.461 ± 7.8c	13.961 ± 3.8b	1.6361 ± 0.18b
A/C/K/Clo30B[b]	44.861 ± 1.6b	75.761 ± 11.5e	14.661 ± 4.4b	1.9561 ± 0.33c

[a] Each value is the mean of three replicates with the standard deviation. Any two means in the same column followed by the same letter are not significantly ($p > 0.05$) different by Duncan's multiple range test.
[b] ACK, agar/κ-carrageenan/konjac glucomannan ternary blend film; Clo30B, Cloisite® 30B.

κ-carrageenan and the agar films. The mechanical properties of the ternary blend film were more close to those of κ-carrageenan film compared with those of the agar or konjac glucomannan films, which made it a fairy strong and stiff film. The ternary blend film was mainly stabilized by physical mixing and the weak interaction such as hydrogen bond and polymer chain-to-chain interaction between component polymer matrices (Kavoosi, Dadfar, & Purfard, 2013). Generally, the mechanical properties of polymer blends are known to be influenced by the interaction or compatibility between the component polymers (Brindle & Krochta, 2008; Rhim, 2012). Usually, compatible polymer blends lead to a significant improvement in mechanical properties, while incompatible polymer blends often lead to inferior mechanical properties (Phan, Debeaufort, Luu, & Voilley, 2009). The TS and E of the ternary blend clay nanocomposite (A/C/K/Clo30B) film increased significantly compared to those of the ternary blend biopolymer (A/C/K) film. It is interesting to note that the TS of the A/C/K/Clo30B film is even higher than that of the κ-carrageenan film. The increase in the mechanical strength has been frequently observed with various biopolymer/clay nanocomposite films (Rhim, 2011, 2012). The increase in TS of the biopolymer/clay nanocomposite films is presumably attributed to the stronger interaction through hydrogen bonds between the polymer matrix and intercalated nanoclay with high surface area and high aspect ratio (Pavlidou & Papaspyrydes, 2008). The distribution of intercalated nanoclay with high elastic modulus generate tremendous interfacial contacts with the polymer matrices, which leads to effective stress transfer resulting in an increase in the TS (Pavlidou & Papaspyrydes, 2008; Rhim, 2012). An agar/Clo30B nanocomposite film prepared by the same procedure used in the present study has been reported to be formed an intercalated nanostructure and exhibited an increase in the TS (Rhim et al., 2011).

3.3. Water vapor permeability (WVP) and water contact angle (CA)

The WVP and the CA values of the films are shown in Table 3. The WVP of agar and κ-carrageenan films were ranged in 1.05–1.15 × 10^{-9} g m/m^2 Pa s, which were much lower than the previously reported values of 1.61–2.01 × 10^{-9} g m/m^2 Pa s (Rhim, 2012). The difference is also caused by the amount of plasticizer used for the preparation of film. Plasticizers are generally known to increase gas, water vapor and solute permeability of the film (Gontard, Guilbert, & Cuq, 1993). The WVP of agar and κ-carrageenan films were significantly ($p < 0.05$) lower than that of konjac glucomannan film. It is seemingly because the konjac glucomannan film is more hydrophilic than the other films, which is evidenced in the result of water contact angle (CA) measurement. The CA, which is one of the basic wetting properties of packaging materials, is usually used as an indicator for hydrophilic/hydrophobic properties of the film surface. The CA values of agar and κ-carrageenan films were 55.1° and 56.1° (Rhim, 2012), and they were higher than previously reported values of 49.3° and 48.1° for agar and κ-carrageenan films, respectively. It is also attributed to the different amount of hydrophilic plasticizer used for the preparation of films. As expected, the konjac glucomannan film showed the lowest CA value indicating that it is more hydrophilic than the other two films. Ternary blend biopolymer (A/C/K) film exhibited in-between WVP values of the component films, which is close to those of CA of agar and κ-carrageenan films. Compared with the A/C/K film, WVP of ternary biopolymer blend nanocomposite (A/C/K/Clo30B) film decreased significantly ($p < 0.05$) after formation of nanocomposite with clay. This is mainly due to the tortuous pathway for water vapor diffusion formed by the impervious nanoclays dispersed in the polymer matrix (Sun, Boo, Clearfield, Sue, & Pham, 2008). On the contrary, the CA of the nanocomposite film was lower than any other films. It is probably because of lower moisture content of the nanocomposite film, which induced rapid water adsorption into the film surface and resulted in lower CA.

3.4. Water solubility (WS), water uptake ratio (WUR), and water vapor uptake ratio (WVUR)

The WS, WUR, and WVUR of agar, κ-carrageenan, konjac glucomannan, and their blend films are shown in Table 4. WS is a measure of the resistance of film against water. The WS of konjac glucomannan film was 100% since it has been completely dissolved in the

Table 3
Water vapor permeability (WVP) and water contact angle (CA) of agar, κ-carrageenan, konjac glucomannan, and their blend films.[a]

Film	MC (%, w.b.)	WVP (×10^{-9} g m/m^2 Pa s)	CA (deg.)
Agar	18.061 ± 0.8c	1.0561 ± 0.07a	55.161 ± 2.0c
κ-Carrageenan	16.261 ± 0.5b	1.1561 ± 0.12ab	56.161 ± 0.8c
Konjac glucomannan	19.361 ± 1.3c	1.4661 ± 0.07c	52.161 ± 2.8b
A/C/K[b]	19.361 ± 0.7c	1.2461 ± 0.01b	54.561 ± 0.8c
A/C/K/Clo30B[b]	13.461 ± 0.2a	1.0461 ± 0.06a	44.061 ± 0.7a

[a] Each value is the mean of three replicates with the standard deviation. Any two means in the same column followed by the same letter are not significantly ($p > 0.05$) different by Duncan's multiple range test.
[b] ACK, agar/κ-carrageenan/konjac glucomannan ternary blend film; Clo30B, Cloisite® 30B.

Table 4
Water solubility (WS), water uptake ratio (WUR), and water vapor uptake ratio (WVUR) of agar, κ-carrageenan, konjac glucomannan, and their blend films.[a]

Film	WS (%)	WUR (%)	WVUR (%)
Agar	14.761 ± 1.0a	79961 ± 43a	46.861 ± 0.2a
κ-Carrageenan	40.961 ± 5.5c	168161 ± 126b	67.361 ± 3.1c
Konjac glucomannan	–[c]	–	63.961 ± 1.6c
A/C/K[b]	16.161 ± 0.7ab	511861 ± 33c	53.861 ± 5.8b
A/C/K/Clo30B[b]	20.361 ± 0.8b	548861 ± 60d	56.161 ± 4.3b

[a] Each value is the mean of three replicates with the standard deviation. Any two means in the same column followed by the same letter are not significantly ($p > 0.05$) different by Duncan's multiple range test.
[b] ACK, agar/κ-carrageenan/konjac glucomannan ternary blend film; Clo30B, Cloisite® 30B.
[c] –, not determined due to disintegration.

water within 15 min of immersion. The WS of κ-carrageenan and agar films were 40.9% and 14.7%, respectively. This result indicates the agar film is the most water resistant followed by κ-carrageenan and konjac glucomannan films. The WS or water resistance of the biopolymer films may be caused by the degree of hydrophilicity of the polymer. On the contrary, the WUR, a measure of water holding capacity of film, showed the reversed order, i.e., the WUR of κ-carrageenan film was about two times more than that of konjac glucomannan film. The WVUR, a measure of water vapor adsorption capacity of film, showed the similar trend as the WUR. The WVUR of κ-carrageenan and konjac glucomannan films was significantly ($p < 0.05$) higher than that of agar film.

Water resistance properties of the biopolymer films have been improved after blending with individual components. Though WS of both ternary blend films (A/C/K and A/C/K/Clo30B) was higher than that of agar film, their WS values were significantly lower than that of κ-carrageenan and konjac glucomannan films. It is noteworthy that the WUR of both ternary blend films increased tremendously up to 5118% and 5488% for A/C/K and A/C/K/Clo30B films, respectively, which means that they can contain more than 50 times of water without disintegration. The WVUR of both the ternary blend films was in the middle range between agar and the other films. The increased water resistance of the ternary blend film can be possibly applied for the food packaging confronting with high humidity condition.

3.5. Water vapor adsorption kinetics and equilibrium moisture content

Water vapor adsorption kinetics of agar, κ-carrageenan, konjac glucomannan, and their blend films was tested at different temperature and RH conditions (10 °C/96% RH, 25 °C/94% RH, and 40 °C/89% RH) and their results are shown in Fig. 1. The water vapor adsorption behaviors of the film samples exhibit characteristic water vapor sorption curves of biopolymer films (Kim & Rhim, 2004). Water vapor adsorption curves of all the film samples showed initial high rate of moisture sorption, then the rate decreased at the later stages until it reached the equilibrium condition. The initial moisture sorption is mainly due to the filling capillaries on the surface of the films (Seog, Zuo, Lee, & Rhim, 2008). As the water vapor sorption proceeded, the sorption rate decreased due to the filling of free capillary with water vapor. Subsequently the curve reached an equilibrium state, at which the maximum water vapor sorption of the film was attained. In all the film samples, the equilibrium state was reached within 24–30 h of water vapor adsorption, and the initial water vapor adsorption rate and the maximum attainable moisture content (i.e., the equilibrium moisture content) were increased with increase in water vapor adsorption temperature. The equilibrium moisture content of the film samples at each condition was determined at extended water vapor adsorption time for more than 53 h which is far beyond the equilibrium state, and the results are shown in Table 5. As expected the equilibrium moisture content (m_e) of all the film samples increased with increase in the adsorption temperature, and κ-carrageenan film showed the highest equilibrium moisture content followed by konjac glucomannan and agar films. The equilibrium moisture content values of the ternary blend films were in-between of agar and κ-carrageenan films. This result is consistent with those of WVUR for the films (Table 4).

The maximum attainable moisture content, i.e., the equilibrium moisture content (m_e), was determined by plotting $1/(m - m_o)$ against $1/t$ using the linearized Singh and Kulshrestha's model. Fig. 2 shows a representative water vapor adsorption data of the ternary blend film. Linear regression lines, drawn through data points, indicate a fairy good fit of the model with high R^2 (the coefficient of determination) values ($R^2 > 0.98$), which confirms the adequacy of the model for describing the water vapor adsorption kinetics of the film sample. The water vapor adsorption data of other film samples were analyzed in the same way and the equilibrium moisture content of the film samples at different temperatures was determined using the linear regression equation, and the results are shown in Table 5. The equilibrium moisture content of films samples determined by using the Singh and Kulshrestha's model were in good agreement with those determined experimentally. This indicates again that the model explains the water vapor adsorption behavior of the films samples (Kim & Rhim, 2004; Seog et al., 2008). In addition, this result also shows that it is not necessary to perform water vapor adsorption test for such an extended time period to determine the equilibrium moisture content of the film.

Table 5
Equilibrium moisture content of agar, κ-carrageenan, konjac glucomannan, and their blend films at different temperatures determined by both experimental and prediction methods.

Film	Temp (°C)	m_e (g H_2O/g DM)		R^2
		Experimental	Predicted	
Agar	10	0.66	0.66	0.98
	25	0.69	0.69	0.98
	40	0.80	0.81	0.98
κ-Carrageenan	10	0.81	0.75	0.94
	25	0.88	0.89	0.99
	40	1.31	1.25	0.95
Konjac glucomannan	10	0.72	0.73	0.99
	25	0.80	0.82	1.00
	40	0.97	0.95	0.99
A/C/K[a]	10	0.62	0.63	1.00
	25	0.72	0.72	0.98
	40	0.95	0.96	0.99
A/C/K/Clo30B[a]	10	0.60	0.60	0.99
	25	0.75	0.74	0.98
	40	0.88	0.88	0.98

[a] A/C/K, agar/κ-carrageenan/konjac glucomannan ternary blend film; Clo30B, Cloisite® 30B.

3.6. Water vapor adsorption isotherm

Water vapor adsorption isotherms of the ternary blend (A/C/K) and the ternary blend nanocomposite (A/C/K/Clo30B) films determined at three different temperatures were determined and the results were shown in Fig. 3. The isotherms of the film samples showed representative sigmoidal curves, in which the equilibrium moisture content (EMC) increased at low water activity ranges up to 0.7, beyond which the EMC increased rapidly. Such pattern of isotherm has been frequently observed with hydrophilic biopolymer films (Perdomo et al., 2009; Zeppa et al., 2009; Rhim, 2011).

The GAB model was fitted to the experimental data and the GAB model parameters were determined using a non-linear regression method. The resulting GAB model parameters with the mean relative percent errors (MRPE) are shown in Table 6. The monolayer moisture content (m_o) of the ternary blend biopolymer films were ranged 0.068–0.075 g water/g dry solid, and it decreased with increase in water vapor sorption temperature. The goodness of fit (MRPE < 5%) indicates the adequacy of the model to fit the experimental data and water vapor isotherm pattern of the film samples (Rhim, 2011; Zeppa et al., 2009). As also observed in the previous tests of WVUR and water vapor adsorption kinetics, the ternary biopolymer blend films exhibited high capacity of adsorbing water vapor. Such biopolymer films with high water vapor adsorption capacity can be properly used as substitute for dehumidifiers like

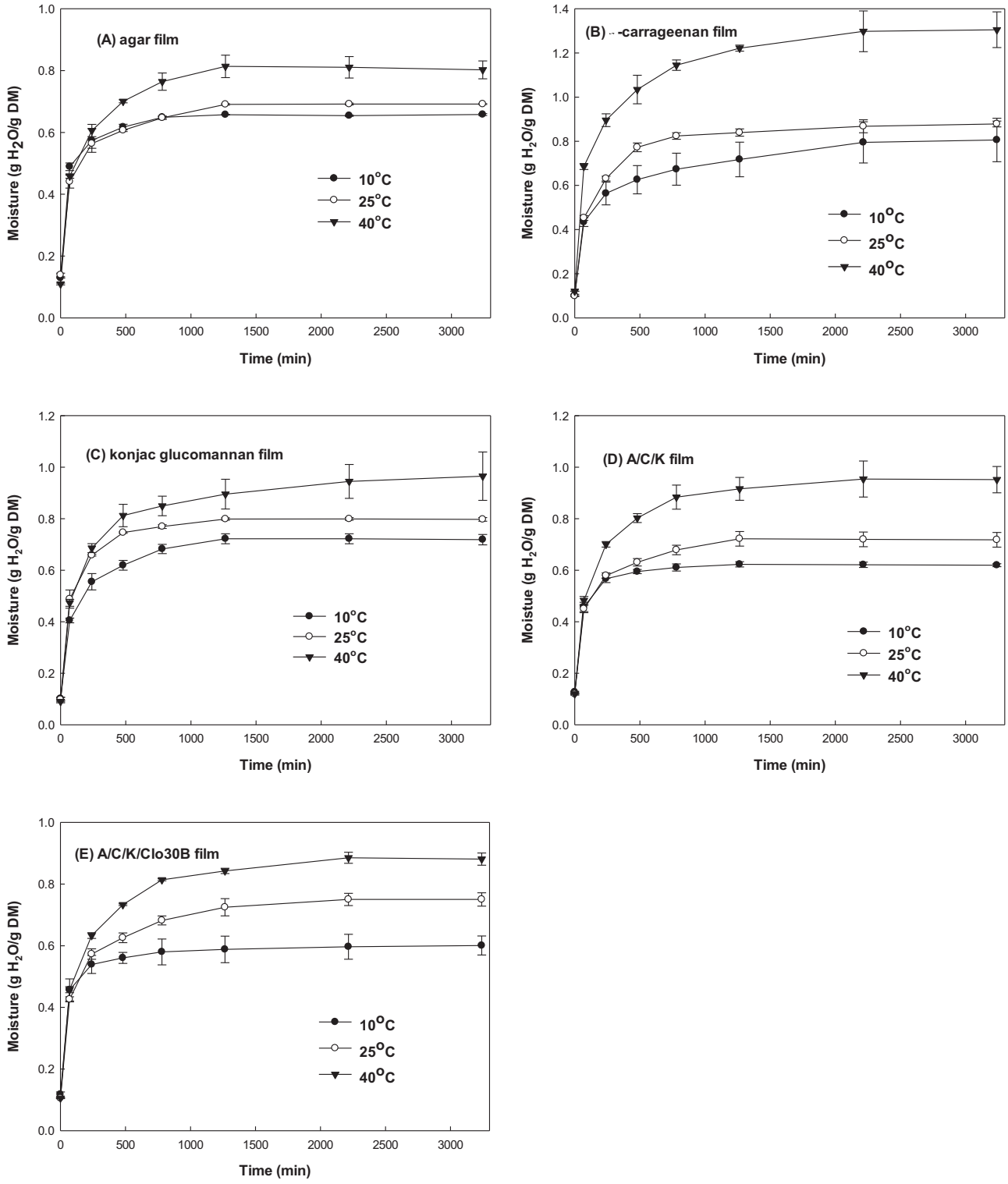

Fig. 1. Change in water vapor adsorption of agar, κ-carrageenan, konjac glucomannan, and their blend films at different temperatures.

silica gel, or as antifogging packaging films for packaging of highly respiring fresh agricultural produce.

3.7. Antimicrobial activity

Antimicrobial activity of the ternary blend biopolymer films has been tested against *L. monocytogenes* and the antimicrobial test result is shown in Fig. 4. As expected, the ternary blend biopolymer film without nanoclay incorporation (A/C/K film) did not show any antimicrobial activity as it exhibited increase in the microbial population with incubation time. On the contrary, the ternary blend biopolymer film incorporated with Cloisite® 30B (A/C/K/Clo30B film) exhibited distinctive antimicrobial activity against test microorganism, in which the microbial population decreased significantly after treating with the film. Such antimicrobial activity has been frequently observed with the Cloisite®

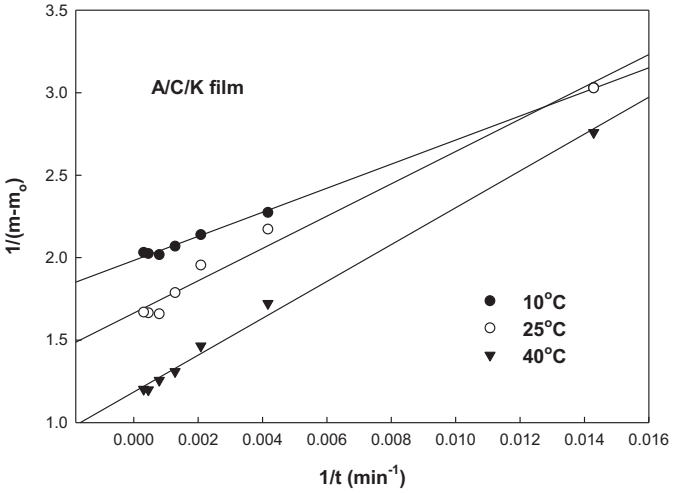

Fig. 2. Water vapor adsorption kinetics of agar/κ-carrageenan/konjac glucomannan (A/C/K) film plotted using a linearized Singh and Kulshrestha's model.

Table 6
GAB model parameters for water vapor adsorption isotherms of agar/κ-carrageenan/konjac glucomannan blend films.

Film	Temp (°C)	C	k	m_o (g H_2O/g DM)	MPRE[a] (%)
A/C/K[b]	10	11.87	0.97	0.074	4.24
	25	7.01	0.98	0.073	4.85
	40	4.80	1.00	0.072	1.63
A/C/K/Clo30B[b]	10	10.35	0.98	0.075	1.18
	25	8.84	0.97	0.075	1.32
	40	8.55	0.97	0.068	2.42

[a] Mean relative percent errors.
[b] A/C/K, agar/κ-carrageenan/konjac glucomannan ternary blend film; Clo30B, Cloisite® 30B.

Table 7
Effect of packaging film on the change in weight of spinach after storage at 5 °C for 5 days.[a]

Packaging film	Weight after storage (g)	Weight loss (%)
No cover	15.7661 ± 2.44c	68.4761 ± 4.88a
LLDPE	49.4261 ± 0.10a	1.1761 ± 0.20c
OPP	47.6661 ± 0.76a	4.6861 ± 1.51c
Perforated OPP	17.2561 ± 2.34c	65.5161 ± 4.69a
A/C/K[b]	45.6361 ± 0.35b	8.7561 ± 0.69b
A/C/K/Clo30B[b]	45.5861 ± 2.14b	8.8461 ± 4.29b

[a] Each value is the mean of three replicates with the standard deviation. Any two means in the same column followed by the same letter are not significantly ($p > 0.05$) different by Duncan's multiple range test.
[b] A/C/K, agar/κ-carrageenan/konjac glucomannan ternary blend film; Clo30B, Cloisite® 30B.

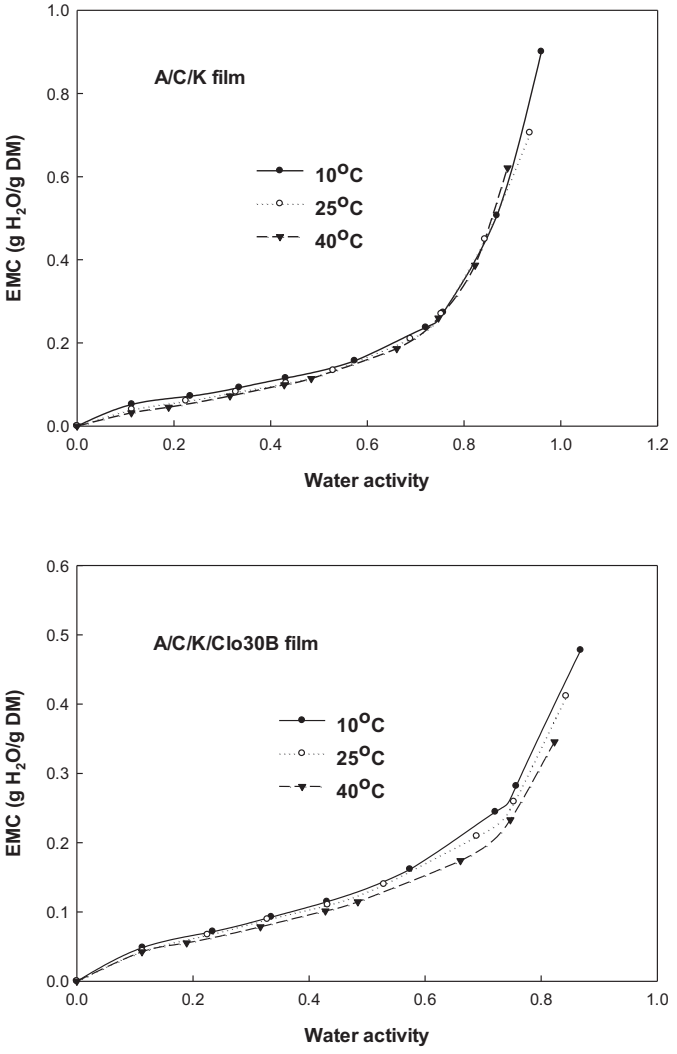

Fig. 3. Water vapor adsorption isotherms of agar/κ-carrageenan/konjac glucomannan (A/C/K) and agar/κ-carrageenan/konjac glucomannan/Cloisite® 30B (A/C/K/Clo30B) films at different temperatures.

30B incorporated biopolymer films including chitosan (Rhim et al., 2006), agar (Rhim et al., 2011), whey protein (Sothornvit, Rhim, & Hong, 2009), and PLA (Rhim, Hong, & Ha, 2009). The antimicrobial activity of the Cloisite® 30B incorporated nanocpmposite films are attributed to the quaternary ammonium salt [i.e., bis-(2-hydroxyethyl)methyl (hydrogenated tallow alkyl) quaternary ammonium] which has been incorporated into the clay for the surface modification of montmorillonite nanoclay (Hong & Rhim, 2008). Such Bio-nanocomposite hydrogels with antimicrobial function can be used in various industries including food packaging and biomedical applications. For example, they can be used in the food packaging industries for extending shelf-life of packaged food and securing the food safety by controlling the growth of post-processing contamination, and in the biomedical industries

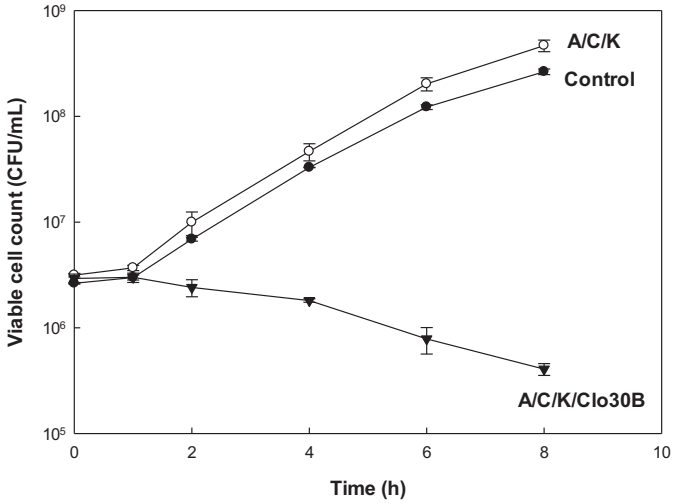

Fig. 4. Antimicrobial activity of agar/κ-carrageenan/konjac glucomannan (A/C/K) and agar/κ-carrageenan/konjac glucomannan/Cloisite® 30B (A/C/K/Clo30B) films against *Listeria monocytogenes*.

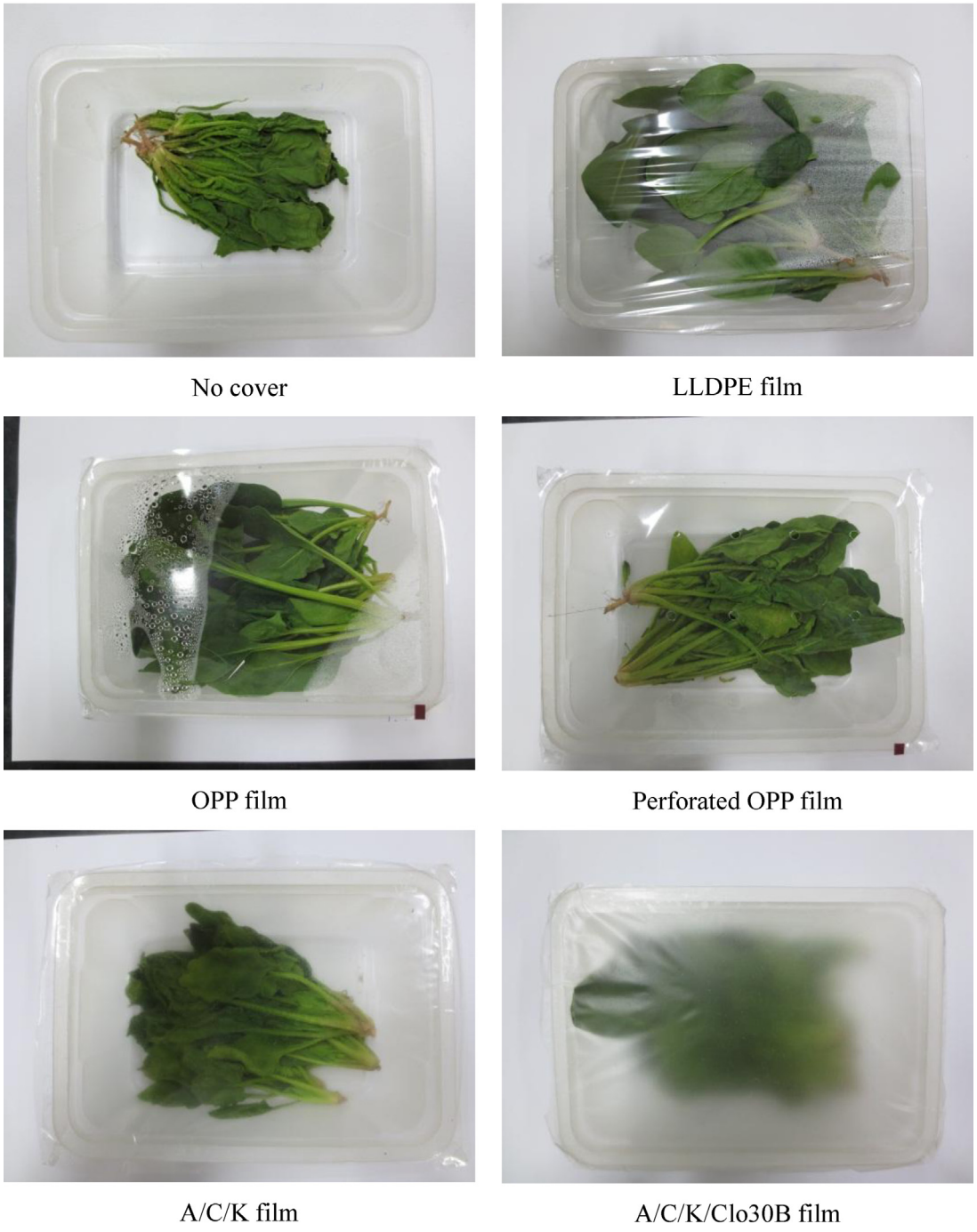

Fig. 5. Effect of packaging materials on formation of water vapor condensation on the surface of packaging film packaged with spinach and stored at 5 °C for 5 days.

for using as wound dressings or skin care bio-hydrogels. However, the antimicrobial activity of the film would be most effective in the condition of direct contact with food or wounded skin.

3.8. Packaging test

The high water vapor adsorptive property of the ternary blend biopolymer films was tested by applying them for packaging of fresh spinach. For the comparison, four more packaging groups including no packaging, commercial wrap (LLDPE), OPP, and perforated OPP packaging, were tested. The appearance of the packages after 5 days of storage at 5 °C is shown in Fig. 5. Spinach sample packed without lid was wilted seriously, and spinach samples packed with LLDPE and OPP film lids were kept fresh shape but water vapor was condensed on the lid films. On the contrary, water drops were not formed on the lids of the perforated OPP, and both of the ternary blend biopolymer films. However, spinach sample packed with the perforated OPP lid was significantly wilted while spinach packed with the ternary blend biopolymer films was kept relatively fresh in shape. Weight loss of spinach sample packaged with different packaging films after storage was determined as shown in Table 6. As expected, the weight loss of spinach without lid was the highest and similar amount of weight loss was observed in the sample covered with perforated OPP film (Table 7). The perforation ratio (1%) of the OPP film seems to be too much to prevent weight loss of the sample. The least weight loss was observed in

spinach sample covered with LLDPE film followed by OPP film. Significant amount of weight loss was observed in the spinach sample covered with both the ternary blend biopolymer films. It is mainly because the water vapor permeability (WVP) of the biopolymer films is much higher than that of the plastic films. Generally, it has been known that the WVP of the plastic films such as LLDPE and OPP is about 4 orders of magnitude lower than that of biopolymer films (Hong & Rhim, 2012). However, the ternary blend biopolymer films were effective to prevent weight loss of spinach, which was comparable to the OPP film. They were also effective to prevent formation of water condensation on the surface of the packaging film.

4. Conclusions

Ternary blend biopolymer hydrogel film and its clay nanocomposite film were developed using hydrogel forming carbohydrates such as agar, κ-carrageenan, and konjac glucomannan powder, and organically modified montmorillonite clay, Cloisite® 30B. The ternary blend films exhibited high water holding and water vapor adsorptive capacity with fairy good water resistance. In addition, the ternary blend nanocomposite film showed significantly improved mechanical and water vapor barrier properties with additional antimicrobial function against Gram-positive bacteria, *L. monocytogenes*. This property of the biopolymer blend films have high potential for the application in the packaging of highly moisture foods or foods contacting with high humidity condition. Preliminary test for packaging of fresh spinach with the developed film revealed that the ternary blend biohydrogel films have a high potential for use as an antifogging packaging film for highly respiring fresh agricultural produce. The high water vapor adsorption capacity of the biohydrogel films suggests that they can be used as desiccant instead of silica gel. The antimicrobial activity of the nanocomposite films prepared with Cloisite® 30B can be used as an active food packaging system for extending the shelf-life of foods and maintaining food quality through controlling the post-processing contamination. They also have a high potential to be applied in the biomedical industry as wound dressings or skin care products.

Acknowledgments

This research was supported by R&D Convergence Center Support Program (710003-03-3-SB320) of the Ministry for Food, Agriculture, Forestry and Fisheries, Republic of Korea.

References

Andersen, F. A. (2005). Amended final report on the safety assessment of polyacrylamide and acrylamide residues in cosmetics. *International Journal of Toxicology*, *24*(Suppl. 2), 21–50.

Bell, L. N., & Labuza, T. P. (2000). Determination of moisture sorption isotherms. In *In moisture sorption: Practical aspects of isotherm measurement and use*. St. Paul, USA: American Association of Cereal Chemists, Inc.14–32.

Berger, J., Reist, M., Chenite, A., Felt-Baeyens, O., Mayer, J. M., & Gurny, R. (2005). Pseudo-thermosetting chitosan hydrogels for biomedical application. *International Journal of Pharmaceutics*, *288*, 17–25.

Billo, E. J. (2007). Nonlinear regression using the solver. In *In Excel® for scientists and engineers: Numerical methods*. Hoboken, NJ: John Wiley & Sons.313–319.

Bordes, P., Pollet, E., & Avérous, L. (2009). Nano-biocomposites: Biodegradable polyester/nanoclay systems. *Progress in Polymer Science*, *34*, 125–155.

Brindle, L. P., & Krochta, J. M. (2008). Physical properties of whey protein-hydroxypropylmethylcellulose blend edible films. *Journal of Food Science*, *79*(9), E446–E454.

Cabedo, L., Feijoo, J. L., Villanueva, M. P., Lagarón, J. M., & Giménez, E. (2006). Optimization of biodegradable nanocomposites based on PLA/PCL blends for food packaging applications. *Macromolecular Symposia*, *233*, 191–197.

De Azeredo, H. M. C. (2009). Nanocomposites for food packaging applications. *Food Research International*, *42*, 1240–1253.

Farris, S., Schaich, K. M., Liu, L., Piergiovanni, L., & Yam, K. L. (2009). Development of polyion-complex hydrogels as an alternative approach for the production of bio-based polymers for packaging applications: A review. *Trends in Food Science & Technology*, *20*, 316–332.

Fernández, A., Picouet, P., & Lloret, E. (2010). Cellulose-silver nanoparticle hybrid materials to control spoilage-related microflora in absorbent pads located trays of fresh-cut melon. *International Journal of Food Microbiology*, *142*, 222–228.

Fernández, E., López, D., López-Cabarcos, E., & Mijangos, C. (2005). Viscoelastic and swelling properties of glucose oxidase loaded polyacrylamide hydrogels and the evaluation of their properties of glucose sensors. *Polymer*, *46*, 2211–2217.

Gennadios, A., Weller, C. L., & Gooding, C. H. (1994). Measurement errors in water vapor permeability of high permeable, hydrophilic edible films. *Journal of Food Engineering*, *21*, 395–409.

Gibas, I., & Janik, H. (2010). Review: Synthetic polymer hydrogels for biomedical applications. *Chemistry & Chemical Technology*, *4*(4), 297–304.

Gontard, N., Guilbert, S., & Cuq, J. L. (1993). Water and glycerol as plasticizers affect mechanical and water vapor barrier properties of an edible wheat gluten film. *Journal of Food Science*, *58*, 206–211.

Hennink, W. E., & van Nostrum, C. F. (2002). Novel crosslinking methods to design hydrogels. *Advanced Drug Delivery Reviews*, *54*, 13–36.

Hong, S. I., & Rhim, J. W. (2008). Antimicrobial activity of organically modified nanoclays. *Journal of Nanoscience and Nanotechnology*, *8*, 5818–5824.

Hong, S. I., & Rhim, J. W. (2012). Preparation and properties of melt-intercalated linear low density polyethylene/clay nanocomposite films prepared by blow extrusion. *LWT-Food Science and Technology*, *48*, 43–51.

Jen, A. C., Wake, M. C., & Mikos, A. G. (1996). Review: Hydrogels for cell immobilization. *Biotechnology and Bioengineering*, *50*, 357–364.

Kavoosi, G., Dadfar, S. M. M., & Purfard, A. M. (2013). Mechanical, physical, antioxidant, and antimicrobial properties of gelatin films incorporated with thymol for potential use as nano wound dressing. *Journal of Food Science*, *78*, E244–E250.

Kim, J. N., & Rhim, J. W. (2004). Kinetics of water vapor adsorption by sweet potato starch-based edible films. *Food Science and Biotechnology*, *13*, 616–621.

Kopeček, J., & Yang, J. (2007). Review hydrogels as smart biomaterials. *Polymer International*, *56*, 1078–1098.

Kundakci, S., Üzüm, B. Ö., & Karadağ, E. (2008). Swelling and dye sorption studies of acrylamide/2-acrylamido-methyl-1-propanesulfonic acid/bentonite highly swollen composite hydrogels. *Reactive & Functional Polymers*, *68*, 458–473.

Liu, Y., & Chan-Park, M. B. (2009). Hydrogel based on interpenetrating polymer networks of dextran and gelatin for vascular tissue engineering. *Biomaterials*, *30*, 196–207.

Luckachan, G. E., & Pillai, C. K. S. (2011). Biodegradable polymers – A review on recent trends and emerging perspectives. *Journal of Polymer and Environment*, *19*, 637–676.

Ma, D., Tu, K., & Zhang, L. M. (2010). Bioactive supramolecular hydrogel with controlled dual drug release characteristics. *Biomacromolecules*, *11*, 2204–2212.

Mateescu, A., Wang, Y., Dostalek, J., & Jonas, U. (2012). Thin hydrogel films for optical biosensor applications. *Membranes*, *2*, 40–69.

Okay, O., Sariişik, S. B., & Zor, S. D. (1998). Swelling behavior of anionic acrylamide-based hydrogels in aqueous salt solutions: Comparison of experiment with theory. *Journal of Applied Polymer Science*, *70*, 567–575.

Öztop, H. N., Hepokur, C., & Saraydin, D. (2009). Acrylamide-sepiolite based composite hydrogels for immobilization of invertase. *Journal of Food Science*, *74*(7), N45–N49.

Pavlidou, S., & Papaspyrydes, C. D. (2008). A review on polymer-layered silicates nanocomposites. *Progress in Polymer Science*, *33*, 1119–1198.

Perdomo, J., Cova, A., Sandoval, A. J., García, L., Laredo, E., & Müller, A. J. (2009). Glass transition temperatures and water sorption isotherms of cassava starch. *Carbohydrate Polymers*, *76*, 305–313.

Phan, T. D., Debeaufort, F., Luu, D., & Voilley, A. (2009). Biopolymer interactions affects the functional properties of edible films based on agar, cassava and arabinoxylan blends. *Journal of Food Engineering*, *90*, 548–558.

Pourjavadi, A., & Barzegar, S. (2009). Synthesis and evaluation of pH and thermosensitive pectin-based superabsorbent hydrogel for oral drug delivery systems. *Starch/Stärke*, *61*, 161–172.

Rhim, J. W., Hong, S. I., Park, H. M., & Ng, P. K. W. (2006). Preparation and characterization of chitosan-based nanocomposite films with antimicrobial activity. *Journal of Agricultural and Food Chemistry*, *54*, 5814–5822.

Rhim, J. W., & Ng, P. K. W. (2007). Natural biopolymer-based nanocomposite films for packaging applications. *Critical Reviews in Food Science and Nutrition*, *47*, 411–433.

Rhim, J. W., Hong, S. I., & Ha, C. S. (2009). Tensile, water vapor barrier and antimicrobial properties of PLA/nanoclay composite films. *LWT-Food Science and Technology*, *42*, 612–617.

Rhim, J. W., Lee, S. B., & Hong, S. I. (2011). Preparation and characterization of agar/clay nanocomposite films: The effect of clay type. *Journal of Food Science*, *76*(3), N40–N48.

Rhim, J. W. (2011). Physical-mechanical properties of agar/κ-carrageenan blend film and derived clay nanocomposite film. *Journal of Food Science*, *76*(8), N67–N74.

Rhim, J. W. (2012). Water vapor adsorption isotherms of agar-based nanocomposite films. *Journal of Food Science*, *77*(12), N68–N72.

Roy, N., Saha, N., Kitano, T., & Saha, P. (2012). Biodegradation of PVP-CMC hydrogel film: A useful food packaging material. *Carbohydrate Polymers*, *89*, 346–353.

Singh, B. P. N., & Kulshrestha, S. P. (1987). Kinetics of water sorption by soybean and pigeonpea grain. *Journal of Food Science*, *52*, 1538–1541, 1544.

Siracusa, V., Rocculi, P., Romani, S., & Rossa, M. D. (2008). Biodegradable polymers for food packaging: A review. *Trends in Food Science and Technology*, *19*, 634–643.

Seog, E. J., Zuo, L., Lee, J. H., & Rhim, J. W. (2008). Kinetics of water vapor adsorption by chitosan-based nanocomposite films. *Food Science and Biotechnology*, *17*, 330–335.

Sothornvit, R., Rhim, J. W., & Hong, S. I. (2009). Effect of nano-clay type on the physical and antimicrobial properties of whey protein isolate/clay composite films. *Journal of Food Engineering*, *91*, 468–473.

Sun, L., Boo, W. J., Clearfield, A., Sue, H. J., & Pham, H. G. (2008). Barrier properties of model epoxy nanocomposites. *Journal of Membrane Science*, *318*, 129–136.

Wang, C. H., Hwang, Y. S., Chiang, P. R., Shen, C. R., Hong, W. H., & Hsiue, G. H. (2012). Extended release of bevacizumab by thermosensitive biodegradable and biocompatible hydrogel. *Biomacromolecules*, *13*, 40–48.

Wu, J., Deng, X., & Lin, X. (2013). Swelling characteristics of konjac glucomannan superabsorbent synthesized by radiation-induced graft copolymerization. *Radiation Physics and Chemistry*, *83*, 90–97.

Xu, J. B., Bartley, J. P., & Johnson, R. A. (2003). Preparation and characterization of alginate hydrogel membranes crosslinked using a water-soluble carbodiimide. *Journal of Applied Polymer Science*, *90*, 747–753.

Yadav, M., & Rhee, K. Y. (2012). Superabsorbent nanocomposite (alginate-g-PAMPS/MMT): Synthesis, characterization and swelling behavior. *Carbohydrate Polymers*, *90*, 165–173.

Yener, Y., & Kalipci, E. (2009). The carcinogenic effects of acrylamide formed during cooking of some foods. *Academic Journal of Cancer Research*, *2*, 25–32.

Yu, H., Xu, X., Chen, X., Hao, J., & Jing, X. (2006). Medicated wound dressings based on poly(vinyl alcohol)/poly(*N*-vinyl pyrrolidone)/chitosan hydrogels. *Journal of Applied Polymer Science*, *101*, 2453–2463.

Zhang, X., Guan, Y., & Zhang, Y. (2012). Ultrathin hydrogel films for rapid optical biosensing. *Biomacromolecules*, *13*, 92–97.

Zhang, X. Z., & Zhuo, R. X. (2002). Synthesis and properties of thermosensitive poly(*N*-isopropylacrylamide-*co*-methyl methacrylate) hydrogel with rapid response. *Materials Letters*, *52*, 5–9.

Zeppa, C., Gouanve, F., & Espuche, E. (2009). Effect of a plasticizer on the structure of biodegradable starch/clay nanocomposites: Thermal, water-sorption, and oxygen-barrier properties. *Journal of Applied Polymer Science*, *112*, 2044–2056.